Energy and exergy analysis of particle dispersed latent heat storage system

S. Jegadheeswaran, S. D. Pohekar

Mechanical Engineering, Tolani Maritime Institute, Induri, Pune 410 507, India.

Abstract
Latent heat thermal storage (LHTS) system has been attractive over the years as an effective energy storage and retrieval device especially in solar thermal applications. However, the performance of LHTS systems is limited by the poor thermal conductivity of phase change materials (PCMs) employed. A numerical study is carried out to investigate the performance enhancement of a LHTS unit of shell and tube configuration due to the dispersion of high conductivity particles in the PCM during charging process (melting). Temperature based governing equations have been formulated and solved numerically following an alternate iteration between the temperature and thermal resistance. Exergy based performance evaluation is taken as a main aspect. The numerical results are presented for several mass flow rates and inlet temperatures of heat transfer fluid (HTF). The results indicate a significant improvement in the performance of the LHTS unit when high conductivity particles are dispersed.
Copyright © 2010 International Energy and Environment Foundation - All rights reserved.

Keywords: Latent heat storage system, Phase change material, Melting, Exergy, Thermal resistance.

1. Introduction
The large scale utilization of the many sources of thermal energy like solar thermal energy, hot waste streams available in industries etc., may be handicapped, if not properly managed. The major problem in managing energy from the above-mentioned sources is the time gap between availability and need. The storage of thermal energy has been emphasized as an attractive solution for such kind of problems on energy management and conservation, in both industrial and domestic sectors. For the last three decades, there has been a growing interest in latent heat thermal storage (LHTS) technique, which has been proved as a better engineering option over sensible heat storage. They offer several advantages such as high energy storage, uniform temperature of operation, simple configuration, etc. In spite of the relative merits, the phase change material (PCM) loaded in the LHTS unit possesses a very low thermal conductivity, which drastically affects the performance of the unit. The various performance techniques proposed and studied are employing fins [1-3], multiple PCMs [4, 5] and increasing the thermal conductivity of conventional PCMs with the help of additives [6-8]. For the recent review on the various performance enhancement techniques employed for LHTS units, readers are referred to the paper by Jegadheeswaran and Pohekar [9]. However, only a limited number of works is reported on dispersion of high conductivity particles, although a large number of studies have focused on other performance enhancement techniques. Seeniraj et al. [6] investigated the effect of high conductivity particles dispersed in the PCM on the performance during the melting process. It is reported that though the

dispersion enhances the performance considerably, there exists an optimum fraction for the particles beyond which, the energy storage capacity would reduce. Khodadadi and Hosseinizadeh [7] have reported that nano copper particles could enhance the heat release rate of PCM (water) significantly during the solidification. Mettawee and Assassa [8] carried out experimental study to investigate the influence of aluminium particles on melting and solidification processes of paraffin used in solar collector. The results revealed that the time required for charging and discharging processes could be reduced substantially by adding the aluminium particles. Hence, the mean daily efficiency of the solar collector with composite PCM was much higher than that of with pure paraffin. The studies on LHTS units employing performance enhancement techniques have mainly focused on evaluation of melting/solidification time, heat transfer rate and amount of energy stored/retrieved in comparison with those of system without enhancement techniques. Recently, Verma et al. [10] have pointed out that thermal analysis of LHTS systems based on only first law of thermodynamics (energy analysis) may not produce a system with highest possible thermodynamic efficiency although workable designs may be possible. This indicates that energy analysis becomes inadequate as information on quality of energy stored/recovered cannot be obtained. In other words, energy analysis does not reflect the usefulness of energy. Hence, an 'optimized LHTS unit' based on first law is not necessarily an optimum system. This inadequacy can be overcome, if an analysis based on second law of thermodynamics (exergy) is carried out for LHTS units. Exergy based performance evaluation of LHTS units has been reported by few researchers [11-14]. To the best of the authors' knowledge, however, exergy analysis is carried out only for multiple PCMs technique [15, 16] and no exergy work is reported for high conductivity particles.

In this work, an attempt is made to study the effect of the dispersion of high conductivity particles on the melting rate and energy /exergy storage in a LHTS unit through mathematical modelling. The comparison between the performance of particle dispersed unit and that of conventional pure PCM charged unit is presented for different mass flow rates and inlet temperatures of HTF.

2. Physical model

The LHTS system consists of a bank of tubes arranged in a particular pattern inside an insulated shell. The shell side is loaded with either pure PCM or PCM dispersed with high conductivity particles and the tube side carries the HTF that flows at a constant inlet temperature higher than the fusion temperature of the PCM. This initiates the melting process. As symmetry is assumed to prevail around a single tube with PCM-particle mix surrounding it, the present analysis has been restricted to the region shown in Figure 1 with the symmetry line taken to be adiabatic. The entire PCM is assumed to be at its fusion temperature (solid phase) initially. The selected materials for PCM and high conductivity particles are technical grade paraffin and copper. The thermophysical properties of PCM [17] and copper [7] are given in Table 1. Water is used as HTF as the system corresponds to that one used for solar water heaters.

Table 1. Thermophysical properties of technical grade paraffin and copper

Properties	Paraffin	Copper
Fusion temperature (K)	300.7	-
Latent heat of fusion (kJ/kg)	206	-
Thermal conductivity (W/m.K)	0.18(solid)/0.19(liquid)	400
Specific heat (kJ/kg.K)	1.8 (solid)/2.4(liquid)	0.383
Density (kg/m^3)	789(solid)/750(liquid)	8954

3. Mathematical modelling

The performance evaluation of LHTS systems requires thorough knowledge of the transient thermal characteristics during the phase change process. Phase change problems are examples of what are closely referred to as moving boundary problems and their study presents one of the most exciting and challenging areas of current applied mathematical research. The existence of a moving boundary generally means that the problem does not admit a simple closed form analytical solution and accordingly much research has focused on approximate solution techniques. In general, phase change problems involve a transient, non-linear phenomenon with a moving liquid-solid interface whose position is unknown a priori and also flow problems associated with HTF. In addition, the two phases of PCM may have different properties and configuration of the LHTS unit may differ with the applications. Substantial number of numerical based studies on LHTS units employing enhancement techniques and

on their performance measurement is available in literature. The numerical formulation widely implemented so far is enthalpy method. However, in the present study a relatively simpler method called alternate temperature and thermal resistance method proposed by Yingqiu et al. [18] has been employed. The details of the mathematical approach are discussed in this section.

3.1 Assumptions
The following assumptions / statements are made to enable the mathematical modelling of the LHTS unit:

- Physical properties of the PCM in both liquid and solid phase are constant and however, may be different for different phases
- Natural convection in the liquid PCM is neglected i.e the heat transfer within PCM is purely by conduction [5]
- As the length of the tube is large compared to its diameter, thermal entrance effects are neglected in the HTF. The flow of HTF is turbulent and fully developed
- No settlement of particles on the tube surface due to density effects
- The particles are in local thermodynamic equilibrium with the surrounding PCM
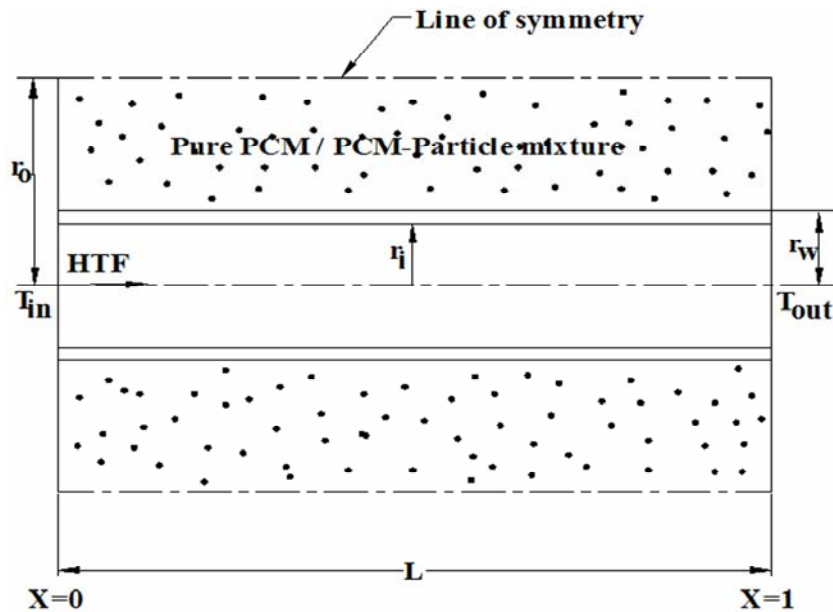
Figure 1. Schematic of LHTS unit

3.2 Formulation
The following equations are arrived by establishing energy balances at the respective regions of HTF, wall and PCM.

$$c_f m_f \frac{\partial T_f(x,t)}{\partial x} = 2\pi r_i h_f [T_f(x,t) - T_w(x,t)] \tag{1}$$

where c_f is the specific heat of HTF (J/kg.K), m_f is the mass flow rate of HTF (kg/s), T_f and T_w are temperatures (K) of HTF and wall respectively, r_i is the tube inner radius (m), h_f is the HTF side heat transfer coefficient (W/m^2.K), x is the axial distance (m), t is the time (s). Since the rate of energy transfer through the tube wall to the PCM is equal to that from HTF to tube wall, we have,

$$\frac{T_f(x,t) - T_w(x,t)}{T_f(x,t) - T_m} = \frac{R_f}{R_f + R_w + R_m(x,t)} \tag{2}$$

where T_m is the fusion temperature of PCM (K), R_f, R_w, R_m are the thermal resistances (K/W) in HTF, wall and PCM respectively.

Rate of change of latent heat stored in a given time interval is equal to the heat convected during that time interval, hence,

$$(1-e)\rho_m H_m \frac{\partial r_{int}(x,t)}{\partial t} = 2\pi r_i h_f [T_f(x,t) - T_w(x,t)] \tag{3}$$

where e is the volume fraction of particles in the PCM, ρ_m is the density of the PCM (kg/m^3), H_m is the latent heat of fusion of PCM (J/kg), r_{int} is the radial interface location (m).

The following initial and boundary conditions are specified in the analysis. Initial conditions:

$$T_f(x, t=0) = T_{in} \tag{4a}$$

where T_{in} is the inlet temperature of HTF (K).

$$r_{int}(x, t=0) = r_w \tag{4b}$$

where r_w is the tube outer radius (m).

Boundary conditions:

$$T_f(x=0, t) = T_{in} \tag{4c}$$

To simplify the formulation, the following dimensionless variables are employed:

$$T_f^* = \frac{T_{in} - T_f}{T_{in} - T_m}; T_w^* = \frac{T_{in} - T_w}{T_{in} - T_m}; X = \frac{x}{L}; r_{int}^* = \frac{r_{int}}{r_o};$$

$$Fo = \frac{\alpha_m t}{r_o^2}; NTU = \frac{h_f 2\pi r_i L}{m_f c_f}; Bi = \frac{h_f r_i}{k_m (or) k_{mix}}; Ste = \frac{c_m (T_{in} - T_m)}{H_m} \tag{4d}$$

where T_f^* and T_w^* are the dimensionless temperatures of HTF and wall respectively, X is the dimensionless axial coordinate, L is the length of the tube (m), r_{int}^* is the dimensionless radial interface location, Fo is the Fourier number, α_m is the thermal diffusivity of PCM (m^2/s), NTU is the number of transfer units, Bi is the Biot number, Ste is the Stefan number, c_m is the specific heat of PCM (J/kg.K), k_m is the thermal conductivity of pure PCM (W/m.K), k_{mix} is the thermal conductivity of PCM-particle mixture (W/m.K) which can be calculated as a function of particle volume fraction as,

$$k_{mix} = k_m \left[\frac{k_p + 2k_m - 2e(k_m - k_p)}{k_p + 2k_m + e(k_m - k_p)} \right] \tag{4e}$$

where k_p is the thermal conductivity of high particles dispersed (W/m.K).

Using the above dimensionless variables, equations (1)-(3) are written in dimensionless form as,

$$\frac{\partial T_f^*(X, Fo)}{\partial X} = (NTU) \left[\frac{R_f}{R_f + R_w + R_m(x,t)} \right] \left(1 - T_f^*(X, Fo)\right) \tag{5}$$

$$\frac{\partial r_{int}^{*2}(X, Fo)}{\partial Fo} = \frac{2Bi}{(1-e)} \left(\frac{k_{mix}}{k_m}\right) Ste \left[\frac{R_f}{R_f + R_w + R_m(x,t)} \right] \left(1 - T_f^*(X, Fo)\right) \tag{6}$$

Equations (5) and (6) and subjected to the following dimensionless initial and boundary conditions, Initial conditions:

$$T_f^*(X, Fo = 0) = 0 \quad \text{for} \qquad\qquad 0 \le X \le 1 \tag{7a}$$

$$r_{\text{int}}^*(X, Fo = 0) = 1 \quad \text{for} \qquad\qquad 0 \le X \le 1 \tag{7b}$$

Boundary conditions:

$$T_f^*(X = 0, Fo) = 0 \quad \text{for} \qquad\qquad Fo > 0 \tag{7c}$$

3.3 Solution

The dimensionless expressions for the axial variation of HTF temperature and interface location at any instant can be easily obtained by integrating equations (5) and (6) with respect to X and Fo respectively and subsequent application of the initial and boundary conditions and are given as follows:

$$T_f^*(X, Fo) = 1 - \exp\left[-NTU \Delta X \sum_{n=i}^{j} \frac{1}{1 + Bi \ln\left(r_{\text{int}}^*(X, Fo)\right) + Bi\left(\frac{k_{mix}}{k_m}\right)\left(\frac{k_m}{k_w}\right)\ln\left(\frac{r_w}{r_i}\right)} \right] \tag{8}$$

$$r_{\text{int}}^*(X, Fo) = \sqrt{1 + \left[\sum_{n=i}^{j} \frac{2Bi}{(1-e)}\left(\frac{k_{mix}}{k_m}\right) Ste \frac{\left(1 - T_f^*(X, Fo)\right)\Delta Fo}{1 + Bi \ln\left(r_{\text{int}}^*(X, Fo)\right) + Bi\left(\frac{k_{mix}}{k_m}\right)\left(\frac{k_m}{k_w}\right)\ln\left(\frac{r_w}{r_i}\right)}\right]} \tag{9}$$

The solution can be obtained by solving the above equations alternatively at each time step until a desired convergence. For the numerical solution, a computational mesh was created with grid size (ΔX) of 0.1. The unsteady analysis was carried out with a time step size of 0.01 s. The grid size and time step were selected after a careful grid and time step independence study. The converged results were assumed to be reached when the relative change between the values of $T_f^*(X, Fo)$ and $r_{\text{int}}^*(X, Fo)$ in subsequent iterations was less than 1×10^{-5}. Initial condition for the iteration is as given in equation (7b).

4. Energy and exergy analysis

At any time, the cumulative energy stored in the PCM is given by,

$$E = \pi/2 \left(r_{\text{int}}^2 - r_w^2\right) L (1-e) \rho_m H_m \tag{10}$$

where E is the cumulative energy stored (J).
Subsequently, the cumulative exergy stored in the PCM at any time can be calculated as follows:

$$Ex_m = E\left[1 - \frac{T_o}{T_m}\right] \tag{11}$$

where Ex_m is the cumulative exergy stored in the PCM(J), T_o is the temperature of environment (K).
The exergy transferred by the HTF can be written as,

$$Ex_f = m_f c_f \left[(T_{out} - T_{in}) - T_o \ln\left(\frac{T_{out}}{T_{in}}\right)\right] \nabla t \tag{12}$$

where Ex_f is the exergy transferred by the HTF (J), T_{out} is the temperature of the HTF at the outlet (K).
The present system studied is assumed as an adiabatic and hence, the heat transferred by the HTF is completely stored in the PCM. As a result, the efficiency of the system becomes unity all the time. Hence, the calculation of energy efficiency does not indicate the true performance of the system. This shortcoming can be overcome, if exergy efficiency is computed.

The exergy efficiency can be expressed as,

$$\psi = \frac{Ex_m}{Ex_f}$$

(13)

where ψ is the exergy efficiency.

5. Results and discussion

The present formulation takes into account the tube wall resistance unlike Yingqiu et al. [18]. For the validation of the computer code, the present results upon setting wall resistance and particle fraction to zero are compared with those of Yingqiu et al. [18]. The comparison is presented in Figure 2 and it is clear from the Figure 2 that the present results agree well with those of Yingqiu et al. [18].
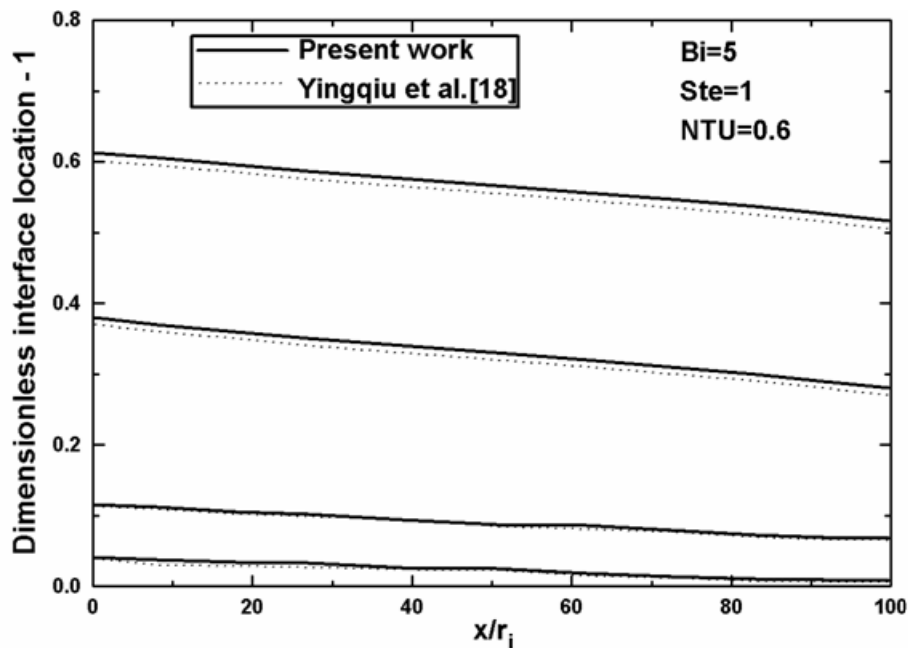
Figure 2. Comparison of interface locations obtained in the present work with that of Yingqiu et al. [18]

In the present study, series of parametric studies were carried out with different design and operating parameters. The identified design and operating parameters are listed in Table 2.

Table 2. Design and operating parameters used in the analysis

Parameter	Value
Inner radius of the tube, r_i (m)	0.0365
Outer radius of the tube, r_w (m)	0.0375
Radius of the shell, r_o (m)	0.075
Length of the unit, L (m)	1
Particle volume fraction, e	0.1,0.2,0.3,0.4,0.5 and 0.6
Biot number, Bi	0.1,0.3,0.5
Stefan number, Ste	0.2,0.3,0.4
Number of transfer units, NTU	0.01
Environment temperature, T_o (K)	298

5.1 Interface location

Figure 3 shows the influence of particle fraction, on the variation of interface location with time. An appreciable increase in dimensionless interface location is obtained with the dispersion of high conductivity particles in the PCM even for a small Biot number. Thus the addition of particles increases

the melting rate due to the increase in heat transfer rate. The influence of particles is more pronounced at the later stages of the melting than at the initial stages. It is seen that at the initial stages of the charging process, the interface location increases about 5 % with $e = 0.1$ and 25 % with $e = 0.4$. As the melting process continues, the growth of the melt layer is enhanced by 29 % with $e = 0.1$ and 72 % with $e = 0.4$. This represents an appreciable enhancement in the heat conduction inside the PCM with dispersed high conductivity particles as time progresses. Similarly, the advancement of the melt layer can be accelerated by increasing the Biot number as well as Stefan number. This can be seen from Figure 4 and Figure 5 respectively. Higher Biot number corresponds to the increase in mass flow rate of HTF and higher Stefan number reflects the increased HTF inlet temperature. Hence, the heat transfer rate increases with the increase of Biot number or Stefan number. However, as it can be seen from Figure 4, the increase in growth of interface is more pronounced between the Biot numbers from 0.1 to 0.3 than between 0.3 to 0.5. The average increment in growth of melt layer is 25% when the Biot number is increased from 0.1 to 0.3 with volume fraction 0.4 and Stefan number 0.2. On the other hand, under the same conditions the increase is around 13% when the Biot number is increased from 0.3 to 0.5. Similar results are observed for the effect of Stefan number on the growth of interface.

The faster growth of interface leads to decrease in the time required for complete melting of the PCM. Hence, the addition of high conductivity particles gives the immediate benefit of reduction in melting time. This is clear from the Table 3 in which the influence of Biot number and Stefan number on the melting time is also presented. As it can be seen, the percentage decrease in melting time increases as the particle fraction increases for all Biot numbers and Stefan numbers. However, beyond a value of 0.3 fraction, no significant increase could be achieved.

Table 3. Percentage decrease in melting time due to addition of particles for various Bi and Ste

	$Ste = 0.2$		$Ste = 0.3$	
	$Bi = 0.1$	$Bi = 0.3$	$Bi = 0.1$	$Bi = 0.3$
$e = 0.1$	47%	48%	48%	48%
$e = 0.2$	73%	72%	73%	73%
$e = 0.3$	81%	81%	81%	81%
$e = 0.4$	85%	86%	86%	86%
$e = 0.5$	88%	88%	88%	88%
$e = 0.6$	90%	90%	90%	90%
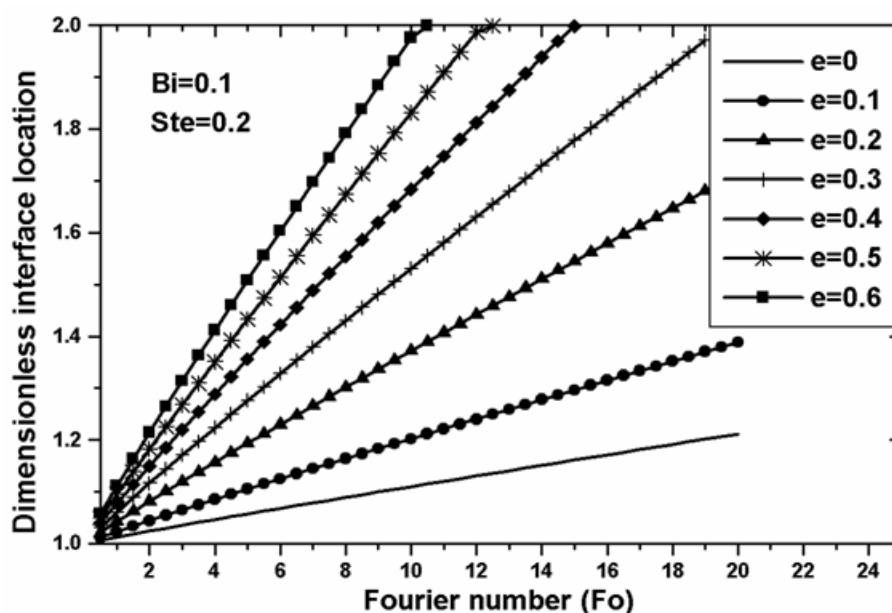
Figure 3. Effect of particle fraction on the time-wise radial interface location
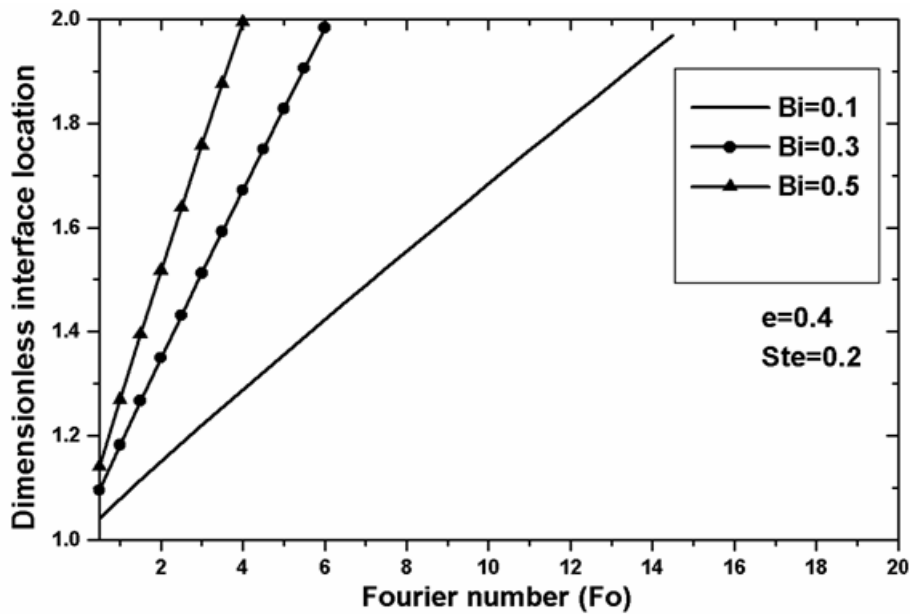
Figure 4. Effect of Biot number on the time-wise radial interface location
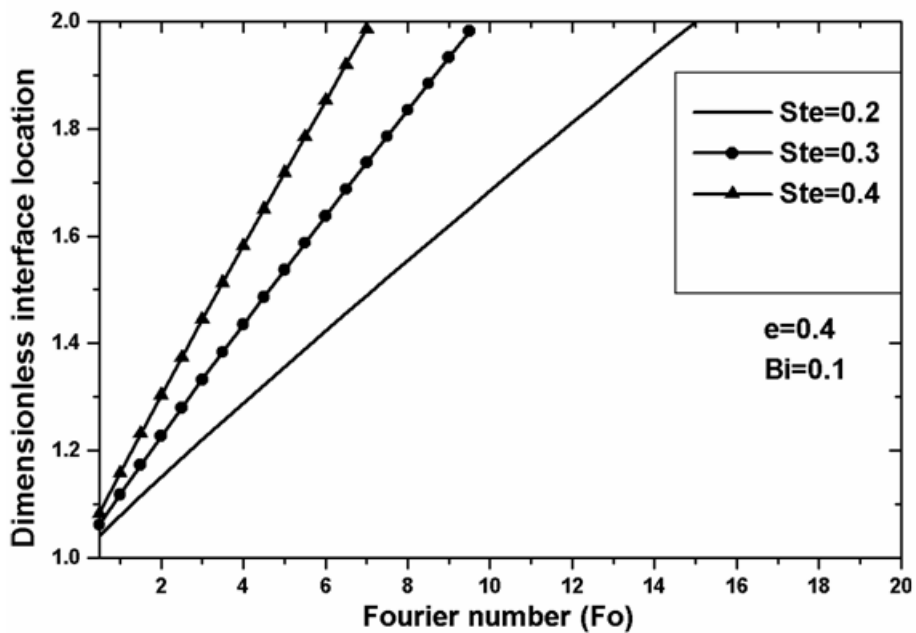
Figure 5. Effect of Stefan number on the time-wise radial interface location

5.2 HTF outlet temperature

The HTF enters the system at a constant inlet temperature (T^*_f =0) and causes the melting. Figure 6 shows the combined effect of particle fraction and Biot number on the time-wise variation of dimensionless HTF outlet temperature. It is seen that for any Biot number and particle fraction, there is continual drop in dimensionless HTF outlet temperature (T^*_{out}) as the time progresses. In the present formulation, the definition of T^*_{out} is such that a decrease in T^*_{out} corresponds to an increase in dimensional temperature of HTF at outlet (T_{out}). At any time, the value of T^*_{out} decreases as the particle fraction increases. Though there is a sudden drop in T^*_{out} in pure PCM case (e = 0) in the beginning, the drop becomes only marginal as the melting progresses. However, the addition of particles could maintain the drop in T^*_{out} considerably through out the process. This means the HTF outlet temperature can be maintained as high as possible by the addition of high conductivity particles. The higher HTF outlet temperature even after storing the energy is beneficial as the application can receive the HTF with minimal temperature drop. It can also be noticed from Figure 6 that no appreciable change in T^*_{out} with

increase in Biot number for any value of particle fraction. This indicates that mass flow rate of HTF does not contribute to the HTF outlet temperature.

The influence of Stefan number on T^*_{out} for various particle fractions is shown in Figure 7. The results indicate that for any particle fraction, the effect of Stefan number at all times is almost negligible. Hence, the contribution of Stefan number to the increase of HTF outlet temperature is negligible even with the presence of high conductivity particles.
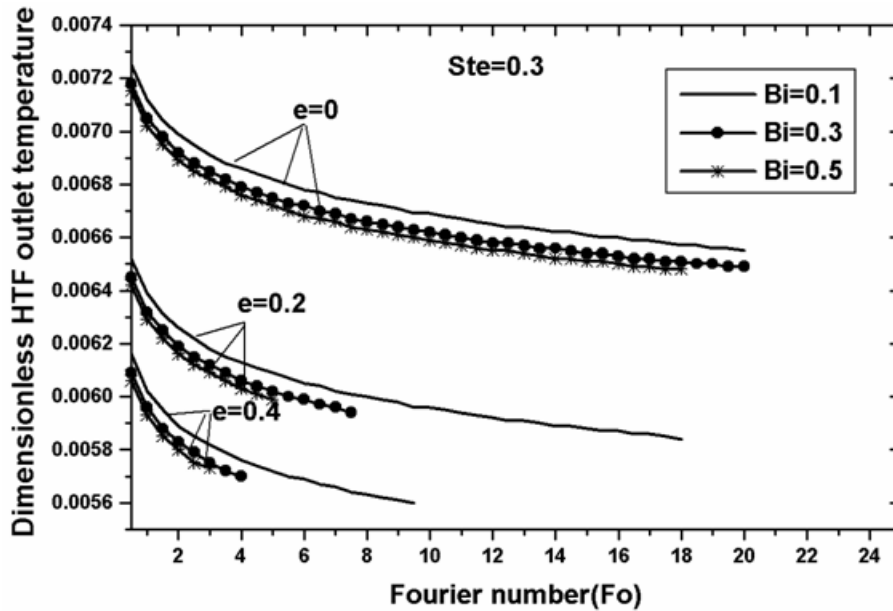
Figure 6. Effect of particle fraction and Biot number on the time-wise dimensionless HTF outlet temperature
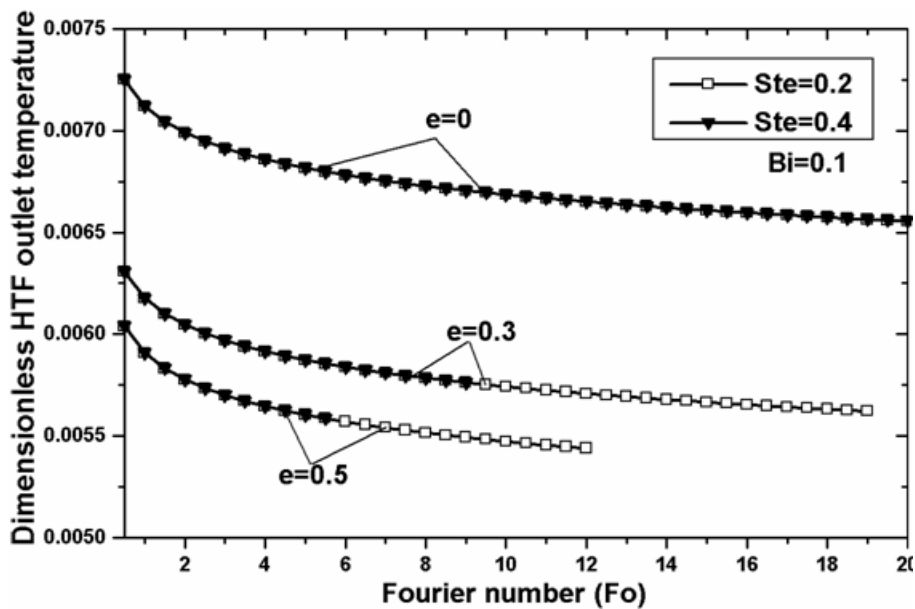
Figure 7. Effect of particle fraction and Stefan number on the time-wise dimensionless HTF outlet temperature

5.3 Cumulative energy stored and exergy stored

It has already been stated that the energy stored in the unit is in the form of latent heat as the sensible heating of the liquid PCM is neglected for the sake of simplifying the analysis. Figure 8 and Figure 9 show the influence of particles as well as the Biot number on the cumulative energy stored and cumulative exergy stored respectively as the melting progresses. It is observed that an appreciable

enhancement in both the energy storage and exergy stored is obtained in the LHTS unit containing dispersed high conductivity particles in the PCM. Also it is noted that combined effect of higher Biot number and particle fraction value results in a higher amount of energy/exergy stored during any time interval. Hence, addition of high conductivity particles and increased HTF mass flow rate not only increase the energy stored but, also the quality of energy stored. The increment of energy storage or exergy storage due to increase in Biot number is observed as consistent for all particle fractions. However, as the particle fraction increases the increase in energy/exergy stored becomes less and less. It should also be mentioned that total amount of energy or exergy stored in the unit after the complete melting decreases as the particle fraction increases. For example, when $Bi = 0.1$ and $Ste = 0.2$, the total amount of both the energy and exergy stored are reduced by 30% with $e = 0.3$ and 50% with $e = 0.5$. This is attributed to the fact that the volume occupied by the PCM is lowered due to the addition of particles.
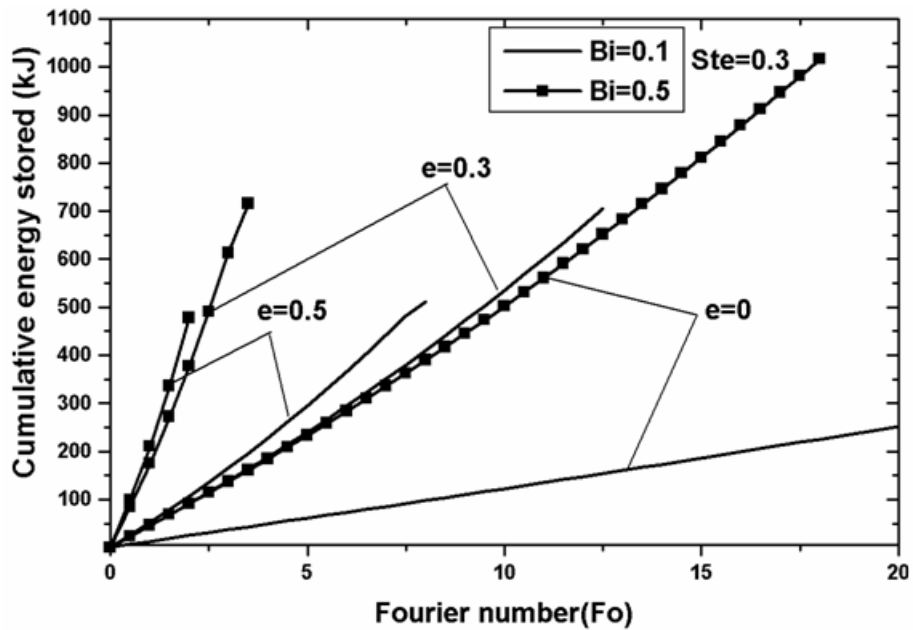
Figure 8. Effect of particle fraction and Biot number on cumulative energy stored
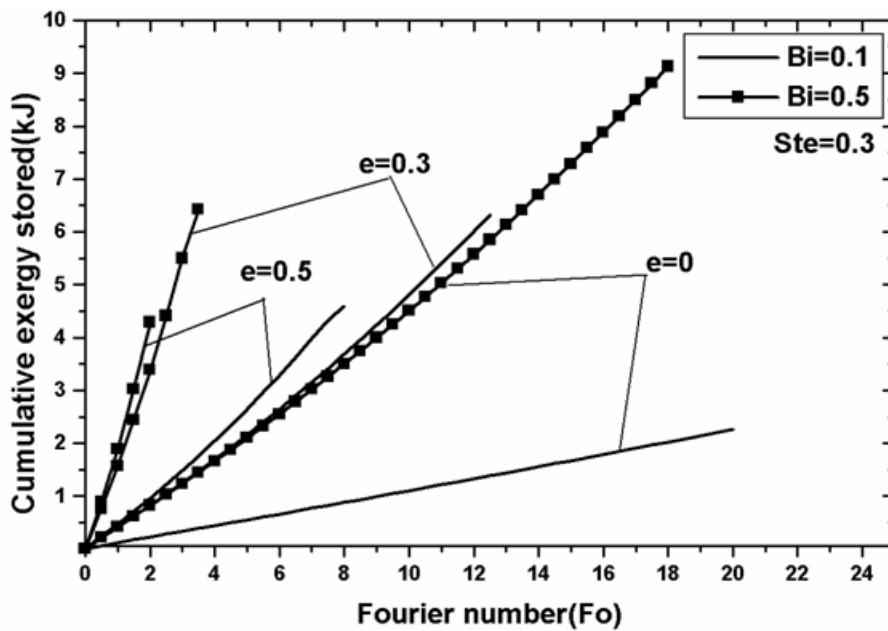
Figure 9. Effect of particle fraction and Biot number on the cumulative exergy stored

The effect of Stefan number on energy storage and exergy storage has also been investigated and the results are presented in Figure 10 and Figure 11. The increase in Stefan number indicates more sensible heat contribution over the latent heat stored in the unit due the higher HTF inlet temperature and thus more energy and exergy stored. However, this increase is appreciable only with lower particle fraction values. For higher particle fractions, the influence of Stefan number seems to be less significant.
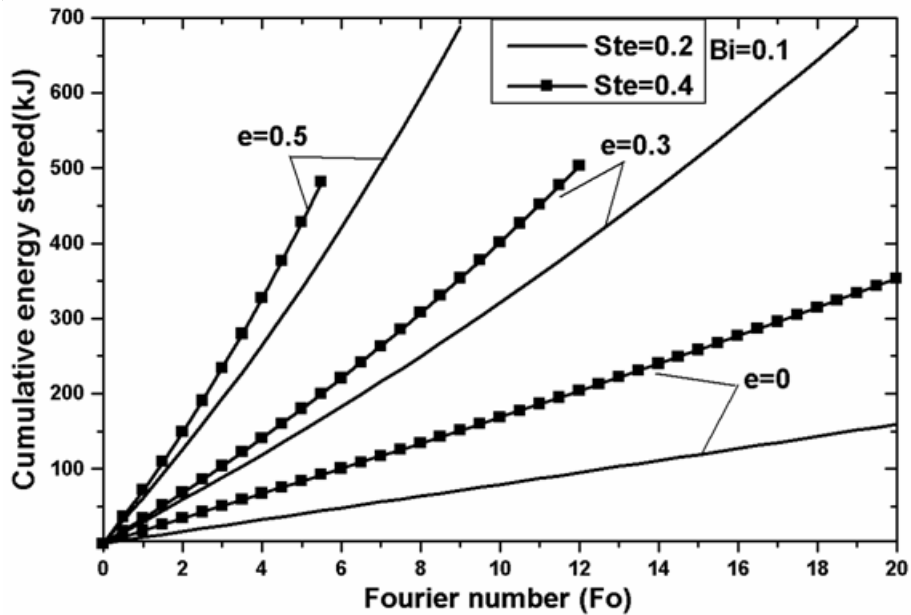
Figure 10. Effect of particle fraction and Stefan number on cumulative energy stored
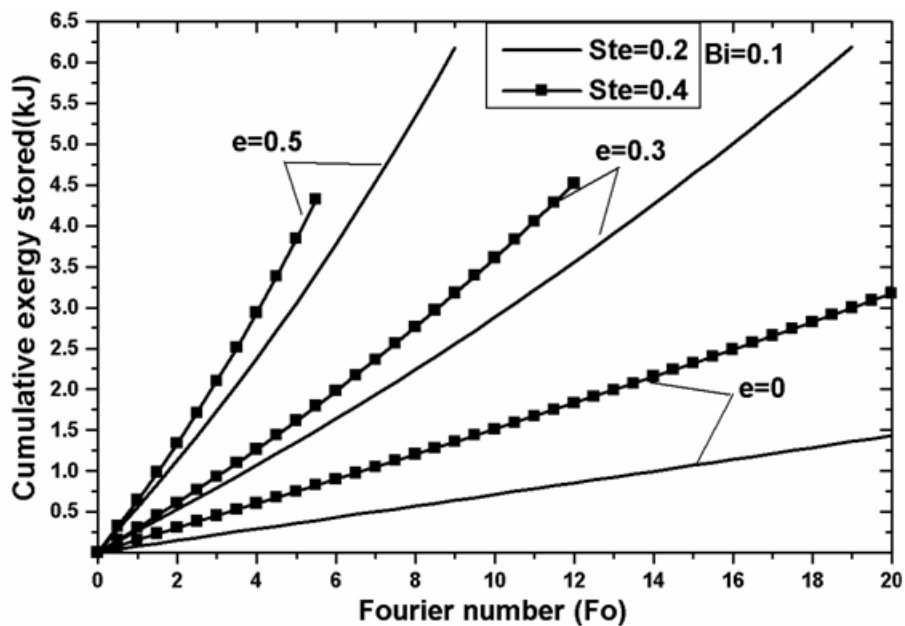
Figure 11. Effect of particle fraction and Stefan number on cumulative energy stored

5.4 Exergy efficiency
The exergy efficiency is introduced in this analysis to measure the internal irreversibilities (entropy generation) which destroy the portion of input exergy. Figure 12 shows the effect of particle fraction and Biot number on the exergy efficiency. For all values of Biot number and particle fraction, the exergy efficiency increases with time. This is due to the fact that the cumulative exergy stored increases as the time advances. The exergy efficiency at any time is increased by addition of particles. In case of pure PCM, the maximum exergy efficiency is only 8% for Bi = 0.1 and Ste = 0.2. Under the same conditions, a maximum efficiency of 15% is possible even with e = 0.1 and it can be as high as 40% with e = 0.5. At any time, the presence of particles in the PCM promotes the heat transfer rate due to the improvement of

thermal conductivity. This results in reduction in irreversibility and thus higher exergy efficiency. Since the increase in Biot number also promotes the heat transfer rate, the exergy efficiency at time is higher for higher Biot numbers. However, the impact of Biot number on exergy efficiency is more pronounced in case of particle dispersed PCM case as compared to pure PCM case. Hence, a combination of higher Biot number and higher particle fraction would lead to reduction in destroyed exergy input.

Figure 13 presents the variation of exergy efficiency under the influence of Stefan number for various particle fractions. At any time and for any particle fraction, the exergy efficiency of the system decreases as the Stefan number increases. As stated earlier, the inlet temperature of the HTF is higher at higher Stefan number. If the inlet temperature of HTF is increased, then the temperature difference at which the heat is transferred remains higher. The heat transfer with higher temperature difference results in more destruction of input exergy. This is the reason why the exergy efficiency remains low for higher Stefan numbers. Moreover, the decrease in exergy efficiency due to increase in Stefan number becomes more and more as the particle fraction is increased. Hence, lower HTF inlet temperature is recommended to enhance the quality of energy stored.
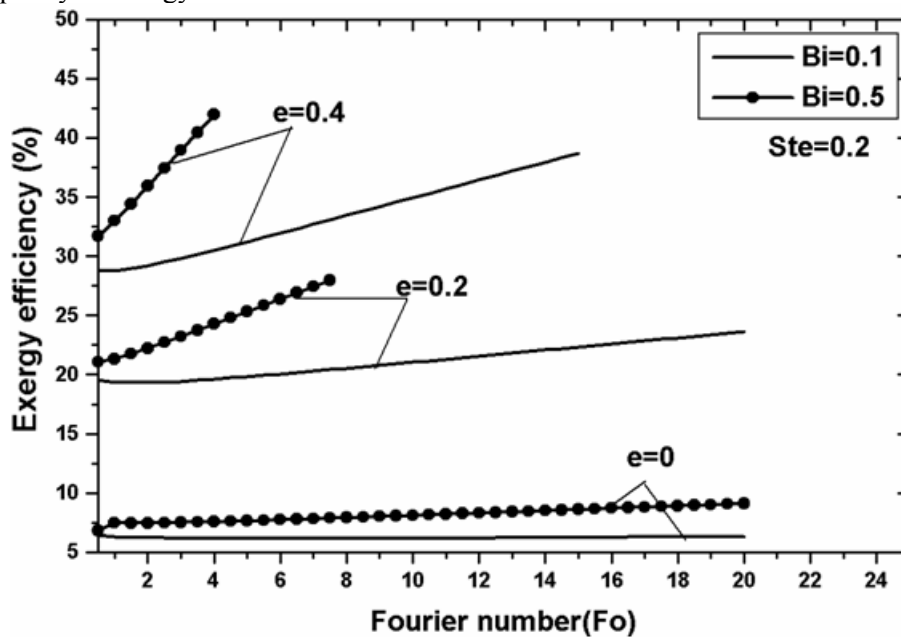
Figure 12. Effect of particle fraction and Biot number on exergy efficiency
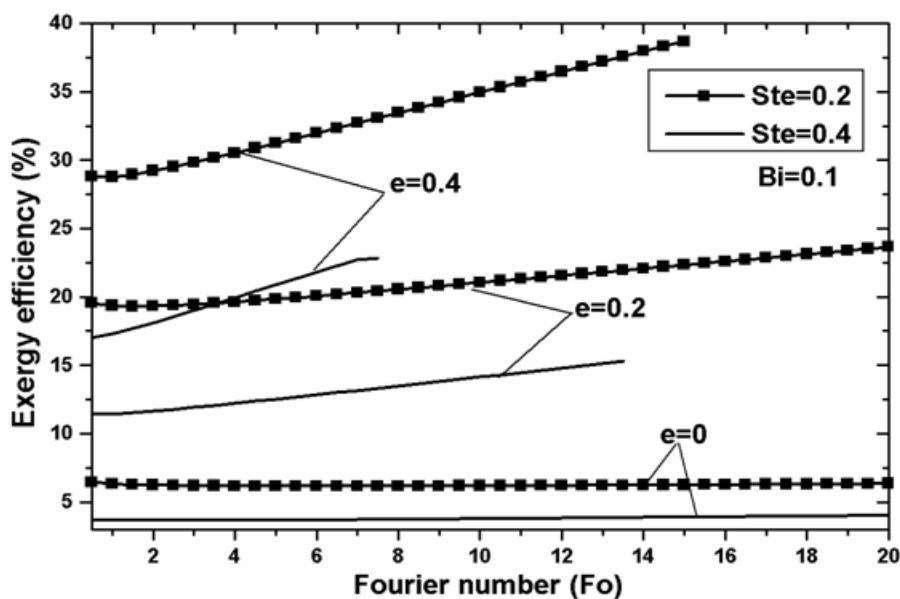
Figure 13. Effect of particle fraction and Stefan number on exergy efficiency

6. Conclusion

In the present work, the performance characteristics of a shell and tube LHTS unit charged with high conductivity particles dispersed PCM during charging mode were investigated numerically. The transient numerical calculations were performed using alternate temperature and thermal resistance method. Exergy analysis was taken as a main aspect in order to assess the performance of the system. From the results obtained, the following conclusions are drawn.

- The addition of high conductivity particles into PCM enhances the melting rate considerably, due to the improvement in the thermal conductivity of PCM. Particle dispersed unit provides better performance also in terms of exergy efficiency as compared to pure PCM unit despite the fact that the total energy or exergy stored is reduced. From thermoeconomics point of view, higher exergy efficiency is always preferred.

- Increasing mass flow rate of HTF also has a significant influence on performance enhancement. Higher mass flow rates along with higher particle fraction would lead to enhanced performance as the system irreversibility could be reduced. However, higher mass flow rates of HTF require high pumping power. Hence, the addition of high conductivity particles is better option than increasing the mass flow rate of HTF.

- Although higher HTF inlet temperatures can enhance the melting rate, the exergy efficiency becomes low as compared to that for lower values. Moreover, operating the system with lower HTF inlet temperature provides less temperature drop.This is preferable from application point of view.

- Exergy based performance evaluation of LHTS system can be stated as more perspective measure than energy based one as it reflects the true potential of the system.

References

[1]   Gharebaghi M., Sezai I. Enhancement of heat transfer in latent heat storage modules with internal fins. Numer. Heat Trans. Part A 2008, 53, 749-765.
[2]   Seeniraj R.V., Velraj R., Lakshmi Narasimhan N. Thermal analysis of a finned tube LHTS module for a solar dynamic power system. Heat Mass Trans. 2002, 38, 409 – 417.
[3]   Shatikian V., Ziskind G., Letan R. Numerical investigation of a PCM-based heat sink with internal fins. Int. J. Heat Mass Trans. 2005, 48, 3689-3706.
[4]   Michels H., Pitz-Paal R. Cascaded latent heat storage for parabolic trough solar power plants. Sol. Energy 2007, 81, 829-837.
[5]   Seeniraj R.V., Lakshmi Narasimhan N. Performance enhancement of a solar dynamic LHTS module having both fins and multiple PCMs. Sol. Energy 2008, 82, 535-542.
[6]   Seeniraj R.V., Velraj R., Lakshmi Narasimhan N. Heat transfer enhancement study of a LHTS unit containing high conductivity particles. J. Sol. Energy Eng. 2008, 124, 243-249.
[7]   Khodadadi J.M, Hosseinizadeh S.F. Nanoparticle-enhanced phase change materials (NEPCM) with great potential for improved thermal energy storage. Int. Comm. Heat Mass Trans. 2007, 34, 534-543.
[8]   Mettawee E.B.S., Assassa E.M.R. Thermal conductivity enhancement in a latent heat storage system. Sol. Energy 2007, 81, 839-845.
[9]   Jegadheeswaran S., Pohekar S.D. Performance enhancement in latent heat thermal storage system: a review. Renew. Sust. Energy Rev. 2009,13, 2225-2244.
[10]   Verma P., Varun., Singal S.K. Review of mathematical modeling on latent heat thermal energy storage systems using phase-change material. Renew. Sust. Energy Rev. 2008, 12, 999-1031.
[11]   Ozturk H.H. Experimental evaluation of energy and exergy efficiency of a seasonal latent heat storage system for green house heating. Energy Convers. Manage. 2005, 46, 1523-1542.
[12]   Kousksou T., Strub F., Lasvignottes J.C., Jamil A., Bedecarrats J.P. Second law analysis of latent thermal storage for solar system. Sol. Energy. Mater. Sol. Cells 2007, 91, 1275-1281.
[13]   Aghbalou F., Badia F., Illa J. Exergetic optimization of solar collector and thermal energy storage system. Int. J. Heat Mass Trans.2006, 49, 1255-1263.

[14] Erek A., Dincer I. A new approach to energy and exergy analyses of latent heat storage unit. Heat Trans. Eng. 2009, 49, 506-525.

[15] Watanabe T., Kanzawa A. Second law optimization of a latent heat storage system with PCMs having different melting points. Heat Recovery Syst. CHP 1995, 15, 641-653.

[16] Domanski R., Fellah G. Exergy analysis for the evaluation of a thermal storage system employing PCMs with different melting temperatures. Appl. Therm. Eng. 1996, 16, 907-919.

[17] Trp A. An experimental and numerical investigation of heat transfer during technical grade paraffin melting and solidification in a shell and tube latent heat thermal energy storage unit. Sol. Energy 2005, 79, 648-660.

[18] Yingqiu Z., Yinping Z., Yi J., Yanbing K. Thermal Storage and Heat Transfer in Phase Change Material Outside a Circular Tube with Axial Variation of the Heat Transfer Fluid Temperature. Int. J. Sol. Energy Eng. 1999, 121,145-149.

S. Jegadheeswaran received his B.E degree in automobile engineering from Institute of Road and Transport Technology, Erode, Tamil Nadu, India in 1993, the M.E degree in thermal engineering from Karunya Institute of Technology, Coimbatore, Tamil Nadu, India in 2004 and is currently pursuing the Ph.D degree in latent heat thermal storage systems for solar thermal applications from Birla Institute of Technology and Science, Pilani, Rajasthan, India. He has published several refereed journal and conference papers concerning latent heat thermal storage systems. His research mainly focuses on performance enhancement and exergy analysis of latent heat thermal storage systems. Mr.Jegadheeswaran is currently serving as assistant professor in Mechanical Engineering at Tolani Maritime Institute, Pune, India.

E-mail address: jdees.2002@gmail.com.

S.D.Pohekar received his B.E degree in mechanical engineering from Govt. College of Engineering, Amravati, Maharashtra, India in 1989, the M.E degree in energy management from Devi Ahilya University, Indore, Madhya Pradesh, India in 1994 and the Ph.D degree in mechanical engineering from Birla Institute of Technology and Science, Pilani, Rajasthan, India in 2004. He has published several refereed journal and conference papers in the areas of energy management and latent heat thermal storage systems. His research interests include multi-criteria decision making and energy storage. Dr.Pohekar is a life member of Solar energy society of India and International society of multi-criteria decision making, and fellow of Institution of Engineers (India) and Maritime Research Institute. He has been reviewer for many international and national journals. He is also the chief editor of Bulletin of Marine Science and Technology. He is currently serving as professor in Mechanical Engineering at Tolani Maritime Institute, Pune, India.

E-mail address: sdpohekar@gmail.com